Mixed-type vector solitons of the N-coupled mixed derivative nonlinear Schrödinger equations from optical fibers

Min Li, Jing-Hua Xiao, Wen-Jun Liu, Pan Wang, Bo Qin, and Bo Tian*

State Key Laboratory of Information Photonics and Optical Communications, and School of Science, Beijing University of Posts and Telecommunications, Beijing 100876, China

(Received 30 July 2012; revised manuscript received 15 January 2013; published 25 March 2013)

We investigate the mixed-type vector solitons of the N-coupled mixed derivative nonlinear Schrödinger (N-CMDNLS) equations from optical fibers. Mixed-type (m-bright-n-antidark or m-bright-n-dark) vector-soliton solutions are derived via the Hirota method. Such vector solitons are found to be independent of the sign of cubic nonlinearity in the N-CMDNLS equations, which is different from the case of the coupled nonlinear Schrödinger equations. The parameter conditions for the shape-preserving and shape-changing collisions of the mixed-type vector solitons are also given by an asymptotic analysis. As an example, the mixed-type vector-soliton collisions in the 3-CMDNLS equations are graphically illustrated. Those results may be useful to the ultrashort-pulse propagation in nonlinear fibers.

DOI: 10.1103/PhysRevE.87.032914 PACS number(s): 05.45.Yv, 42.65.Tg, 42.81.Dp, 02.30.Ik

I. INTRODUCTION

Vector-soliton propagation and collision properties have been studied intensively due to their applications in optical communication systems [1]. In contrast to scalar solitons, vector solitons have multiple distinct polarization components that can copropagate as one unit without splitting because of the nonlinear effects [2,3]. One phenomenon associated with the collisions of vector solitons is the energy exchange among the components [4–7]. Due to such collision properties and robustness against external perturbations, vector solitons have been applied to the design of such devices as optical switches, signal routers, and data storage [8,9]. So far, three types of vector solitons have been found in the 2-coupled nonlinear Schrödinger (2-CNLS) equations, i.e., the bright vector solitons (both components are bright solitons), dark vector solitons (both components are dark ones), and mixed-type vector solitons (some components are bright while others are dark) [10–14]. In addition, vector solitons of the 2-coupled mixed derivative nonlinear Schrödinger (2-CMDNLS) equations have been studied because of their applications in the femtosecond regime of birefringent optical fibers [15]. Bright, dark, and antidark vector solitons of the 2-CMDNLS equations have been obtained [16,17]. Here antidark solitons exist in the form of a bright pulse on a nonzero continuous-wave background [18].

However, studies on the mixed-type vector solitons for the general N-CMDNLS equations have not yet been proposed. In the present paper we investigate the N-CMDNLS equations [19]

$$iq_{j,t}+q_{j,xx}+\mu\left[\left(\sum_{\eta=1}^{N}\rho_\eta|q_\eta|^2\right)q_j\right]+i\gamma\left[\left(\sum_{\eta=1}^{N}\rho_\eta|q_\eta|^2\right)q_j\right]_x=0\quad(j=1,\ldots,N),\qquad(1)$$

where x and t are the normalized time and distance, respectively, μ and γ are the real constants that denote the measure of cubic nonlinear strength and derivative cubic nonlinearity, ρ_l ($l=1,\ldots,N$) can be either 1 or -1, and q_j represents the slowly varying complex envelopes for the polarizations [19]. The last terms in Eq. (1) contain the self-steepening effect, which plays an important role in the ultrashort-pulse propagation in long optical fibers [20,21]. Equation (1) has been found to possess integrability in the sense of the scattering transform [19]. In the case of $\gamma=0$, Eq. (1) can be reduced to the N-CNLS equations, which arise in optical fibers [21], biophysics [22], Bose-Einstein condensates [23], and plasma physics [24]. When $\mu=0$, Eq. (1) reduces to the N-coupled derivative nonlinear Schrödinger (N-CDNLS) equations, which govern polarized Alfvén waves in plasma physics [25]. Therefore, Eq. (1) can be regarded as a combination of the N-CNLS and N-CDNLS equations. The case $N=2$ in Eq. (1) corresponds to the 2-CMDNLS equations for the two polarized components of the electric field in birefringent optical fibers, which can exhibit a complete or partial energy exchange in the collisions of the bright vector solitons [16]. However, for the dark or antidark vector solitons of the 2-CMDNLS equations, Ref. [17] has shown that no energy transfer happens between the two polarization components. More on the soliton collisions can be seen, e.g., in Refs. [26,27].

The structure of this paper is arranged as follows. Although the bilinear equations of the 2-CMDNLS equations have been presented [16,17], more general ones of the N-CMDNLS equations need to be given. In Sec. II, using the Hirota method [28,29] and symbolic computation [30,31], the bilinear equations and mixed-type vector-soliton solutions of Eq. (1) are obtained. A characteristic analysis of the mixed-type vector-soliton solutions is presented in Sec. III. Parameter conditions are derived to obtain different types of vector-soliton solutions. More importantly, conditions for the shape-preserving and shape-changing collisions of the mixed-type vector solitons are given. Mixed-type vector-soliton collisions of the 3-CMDNLS equations are illustrated in Sec. IV. Numerical simulations of the mixed-type vector solitons are performed

*Corresponding author: tian.bupt@yahoo.com.cn

by virtue of the time-splitting spectral (TSS) method in Sec. V. Finally, a summary and discussion are given in Sec. VI.

II. MIXED-TYPE VECTOR-SOLITON SOLUTIONS OF EQ. (1)

Soliton solutions, in particular multisoliton solutions, can be derived through the truncated formal perturbation expansion at different levels in bilinear equations [32,33]. In this section we use the Hirota method to obtain the m-bright-n-dark or m-bright-n-antidark ($m+n=N$) vector-soliton solutions of Eq. (1).

By introducing the gauge transformation

$$q_j = u_j \exp\left[-\frac{i\gamma}{2}\int\left(\sum_{\eta=1}^{N}\rho_\eta|u_\eta|^2\right)dx\right] \quad (j=1,\ldots,N), \tag{2}$$

we transform Eq. (1) into the form

$$iu_{j,t}+u_{j,xx}+\mu\left[\left(\sum_{\eta=1}^{N}\rho_\eta|u_\eta|^2\right)u_j\right] + i\gamma\left(\sum_{\eta=1}^{N}\rho_\eta u_{\eta,x}u_\eta^*\right)u_j=0 \quad (j=1,\ldots,N), \tag{3}$$

where the asterisk denotes the complex conjugate. Through the rational dependent-variable transformations

$$u_s=\frac{g_s}{f} \quad (s=1,2,\ldots,m), \tag{4a}$$

$$u_{m+l}=\frac{h_l}{f} \quad (l=1,2,\ldots,n), \tag{4b}$$

where $g_s(x,t)$ $(s=1,\ldots,m)$, $h_l(x,t)$ $(l=1,\ldots,n)$, and $f(x,t)$ are all complex functions to be determined, Eq. (3) can be bilinearized as

$$\left(iD_t+D_x^2-\lambda\right)(g_s\cdot f)=0 \quad (s=1,\ldots,m), \tag{5}$$

$$\left(iD_t+D_x^2-\lambda\right)(h_l\cdot f)=0 \quad (l=1,\ldots,n), \tag{6}$$

$$D_x(f^*\cdot f)=-\frac{i\gamma}{2}\left(\sum_{s=1}^{m}\rho_s|g_s|^2+\sum_{l=1}^{n}\rho_{m+l}|h_l|^2\right), \tag{7}$$

$$\left(D_x^2-\lambda\right)(f^*\cdot f) =\mu\left(\sum_{s=1}^{m}\rho_s|g_s|^2+\sum_{l=1}^{n}\rho_{m+l}|h_l|^2\right) -\frac{i\gamma}{2}\left[\sum_{s=1}^{m}\rho_s D_x(g_s^*\cdot g_s)+\sum_{l=1}^{n}\rho_{m+l}D_x(h_l^*\cdot h_l)\right], \tag{8}$$

where λ is a real constant to be determined, and the bilinear operators D_t and D_x are defined by [32]

$$D_x^m D_t^n(f\cdot g) =\left(\frac{\partial}{\partial x}-\frac{\partial}{\partial x'}\right)^m\left(\frac{\partial}{\partial t}-\frac{\partial}{\partial t'}\right)^n f(x,t)g(x',t')\big|_{x'=x,t'=t},$$

with x' and t' as the formal variables. Note that Eq. (1) can be obtained from Eqs. (5)–(8) with the choice of $q_j=u_j f^*/f$ $(j=1,\ldots,N)$ due to the gauge equivalence between Eqs. (1) and (3). Then Eqs. (5)–(8) can also be seen as the bilinear equations of Eq. (1). Moreover, Eqs. (5)–(8) are more general than those obtained in Ref. [16] because they can reduce to the bilinear equations of the N-CNLS equations in the case of $\gamma=0$ and f being a real function.

In order to obtain the m-bright-n-dark or m-bright-n-antidark vector-soliton solutions of Eq. (1), we expand g_s $(s=1,\ldots,m)$, h_l $(l=1,\ldots,n)$, and f with respect to a formal expansion parameter ε as follows:

$$g_s=\varepsilon g_s^{(1)}+\varepsilon^3 g_s^{(3)}+\varepsilon^5 g_s^{(5)}+\cdots \quad (s=1,\ldots,m), \tag{9}$$

$$h_l=h_l^{(0)}\left(1+\varepsilon^2 h_l^{(2)}+\varepsilon^4 h_l^{(4)}+\cdots\right) \quad (l=1,\ldots,n), \tag{10}$$

$$f=f^{(0)}(1+\varepsilon^2 f^{(2)}+\varepsilon^4 f^{(4)}+\cdots), \tag{11}$$

where $g_s^{(J)}$ $(J=1,3,5,\ldots)$, $h_l^{(L)}$, and $f^{(L)}$ $(L=0,2,4,\ldots)$ are all complex functions to be determined. Substituting expansions (9)–(11) into Eqs. (5)–(8) and truncating the perturbation expansion at different levels, we obtain the mixed-type vector one-soliton and multisoliton solutions of Eq. (1) (see the Appendix).

III. ANALYSIS OF THE MIXED-TYPE VECTOR-SOLITON SOLUTIONS

A. Quantitative analysis of solutions (A7)

It is noted that solution (A7a) can present only one type of soliton solution, i.e., a bright-soliton solution, while solution (A7b) can be a dark- or antidark-soliton solution under different parameter conditions. From solution (A7b) we can see that the sign of Δ_1 ($\Delta_1=\sigma_1+\sigma_1^*-\varrho_{l,1}-\varrho_{l,1}^*$) determines the type of soliton solution. For $\Delta_1>0$, solution (A7b) is a dark-soliton solution, while it will take the form of an antidark-soliton solution in the case of $\Delta_1<0$.

After calculation of Δ_1 with $k_1=k_{1R}+ik_{1I}$ (the suffixes R and I denote the real and imaginary parts), we have

$$\Delta_1=\frac{(-8k_{1I}\gamma+4\mu+3\gamma^2\Theta)\sum_{s=1}^{m}\rho_s|\chi_{s,1}|^2}{8\left(k_{1R}^2+k_{1I}^2\right)+\Theta(-8k_{1I}\gamma+4\mu+3\gamma^2\Theta)}. \tag{12}$$

It is found that ρ_η $(\eta=1,\ldots,m)$ is not the determinate factor for the sign of $\sum_{s=1}^{m}\rho_s|\chi_{s,1}|^2$. As a result we assume $\rho_\eta=1$ $(\eta=1,\ldots,m)$ and $\gamma>0$ (for other cases, the analysis can be performed in a similar way). Then solution (A7b) can exhibit two types of soliton solutions under the following parameter

conditions: For $\mu\Theta < \frac{-8k_{1R}^2-\Theta^2\gamma^2}{4}$,

$$\text{antidark-soliton solutions}: \quad k_{1I} > \frac{3\Theta\gamma^2+4\mu}{8\gamma}, \quad k_{1I} < \frac{\Gamma_1}{4} \text{ or } k_{1I} > \frac{\Gamma_2}{4}, \tag{13}$$

$$\text{dark-soliton solutions}: \quad \begin{aligned} &k_{1I} < \frac{3\Theta\gamma^2+4\mu}{8\gamma}, \quad k_{1I} < \frac{\Gamma_1}{4} \text{ or } k_{1I} > \frac{\Gamma_2}{4} \\ &k_{1I} > \frac{3\Theta\gamma^2+4\mu}{8\gamma}, \quad \frac{\Gamma_1}{4} < k_{1I} < \frac{\Gamma_2}{4}, \end{aligned} \tag{14}$$

with

$$\Gamma_1 = 2\Theta\gamma - \sqrt{2}\sqrt{\Psi}, \quad \Gamma_2 = 2\Theta\gamma + \sqrt{2}\sqrt{\Psi},$$
$$\Psi = -8k_{1R}^2 - \Theta^2\gamma^2 - 4\Theta\mu,$$

and for $\mu\Theta > \frac{-8k_{1R}^2-\Theta^2\gamma^2}{4}$,

$$\text{antidark-soliton solutions}: \quad k_{1I} > \frac{3\Theta\gamma^2+4\mu}{8\gamma}, \tag{15}$$

$$\text{dark-soliton solutions}: \quad k_{1I} < \frac{3\Theta\gamma^2+4\mu}{8\gamma}, \tag{16}$$

where k_{1R} represents a half-wave number, k_{1I} correlates with the velocity of the vector soliton, and ρ_{m+l} $(l = 1, \ldots, n)$ is the sign of nonlinearity. Therefore, with the choices of parameters under conditions (13)–(16), solutions (A7) can describe the propagation of m-bright-n-antidark or m-bright-n-dark ($m + n = N$) vector solitons.

For the CNLS equations, the sign of the nonlinear coefficients determines whether the model is focusing, defocusing, or mixed type [10]. As shown in Refs. [10–14], the bright-dark vector solitons exist only in the CNLS equations with all the nonlinearities being defocusing or mixed focusing and defocusing. Whether the case of Eq. (1) is similar to that of the CNLS equations needs further analysis. Based on the above analysis, bright solitons in the q_s $(s = 1, \ldots, m)$ component can be described by solution (A7a) with any choice of ρ_η $(\eta = 1, \ldots, m)$. Under conditions (13) and (14), to describe the dark-antidark solitons in the q_{m+l} $(l = 1, \ldots, n)$ component, we must require the cubic nonlinear coefficient $\mu\rho_{m+l}$ $(l = 1, \ldots, n)$ to be negative when $n = 1$. However, under conditions (15) and (16), the sign of $\mu\rho_{m+l}$ $(l = 1, \ldots, n$ and $n \geqslant 1)$ can be arbitrary and does not affect the types of solitons. Therefore, the mixed-type vector solitons of Eq. (1) can be obtained for any kind of combination of nonlinearities, which is different from that of the CNLS equations [10,13].

In addition, the propagation characters of solitons can be measured by the velocity, width, amplitude, and initial phase of the envelopes. From solutions (A7), we find that solitons in the q_s $(s = 1, \ldots, m)$ and q_{m+l} $(l = 1, \ldots, n)$ components have the same velocity, width, and initial phase, which are, respectively, $2k_{1I} - \Theta\gamma/2$, $1/(2c_1)$, and $-\ln|\sigma_1|/(2c_1)$. The amplitudes of solitons in the q_s $(s = 1, \ldots, m)$ component can be expressed as $A_s = |\chi_{s,1}|/\sqrt{\sigma_1 + \sigma_1^* + 2|\sigma_1|}$, while the amplitude or depth (corresponding to the antidark or dark soliton, respectively) of solitons in the q_{m+l} $(l = 1, \ldots, n)$ component can be described by $A_{m+l} = |\alpha_l|\sqrt{(\sigma_1 + \sigma_1^* - \varrho_{l,1} - \varrho_{l,1}^*)/(\sigma_1 + \sigma_1^* + 2|\sigma_1|)}$.

B. Asymptotic analysis of solutions (A9)

In the following, we will make the appropriate asymptotic analysis on Solutions (A9) to reveal the dynamics of shape-preserving and shape-changing collisions of solitons among N components (see Appendix). Comparing expressions (A10b) and (A12b), and (A11b) and (A13b), we find that the physical quantities of solitons in the q_{m+l} $(l = 1, \ldots, n)$ component do not change before and after collision except for a small phase shift. This means that the collisions between two solitons are all shape preserving and there is no energy transfer in the last n components, which also indicates that there is no energy exchange between the solitons in the q_s $(s = 1, \ldots, m)$ and q_{m+l} $(l = 1, \ldots, n)$ components. However, comparing expressions (A10a) and (A12a), and (A11a) and (A13a), it can be found that the energy exchange exists among the solitons in the first m components during the interacting process. Specifically, if $\chi_{s_1,2}/\chi_{s_1,1} = \chi_{s_2,2}/\chi_{s_2,1}$ $(s_1 \neq s_2,\ 1 \leqslant s_1$, and $s_2 \leqslant m)$, the collisions between two solitons in the first m components will be shape preserving. On the contrary, the shape-changing collisions between two solitons with energy transfer in the first m components will take place under the condition $\chi_{s_1,2}/\chi_{s_1,1} \neq \chi_{s_2,2}/\chi_{s_2,1}$ $(s_1 \neq s_2$, and $1 \leqslant s_1, s_2 \leqslant m)$.

IV. MIXED-TYPE VECTOR-SOLITON COLLISIONS

For simplicity, we will consider the set of 3-CMDNLS equations by taking $N = 3$ in Eq. (1), i.e.,

$$\begin{aligned} &iq_{1,t} + q_{1,xx} + \mu[(|q_1|^2 + |q_2|^2 + |q_3|^2)q_1] \\ &\quad + i\gamma[(|q_1|^2 + |q_2|^2 + |q_3|^2)q_1]_x = 0, \end{aligned} \tag{17a}$$

$$\begin{aligned} &iq_{2,t} + q_{2,xx} + \mu[(|q_1|^2 + |q_2|^2 + |q_3|^2)q_2] \\ &\quad + i\gamma[(|q_1|^2 + |q_2|^2 + |q_3|^2)q_2]_x = 0, \end{aligned} \tag{17b}$$

$$\begin{aligned} &iq_{3,t} + q_{3,xx} + \mu[(|q_1|^2 + |q_2|^2 + |q_3|^2)q_3] \\ &\quad + i\gamma[(|q_1|^2 + |q_2|^2 + |q_3|^2)q_3]_x = 0, \end{aligned} \tag{17c}$$

with $\rho_\eta = 1$ $(\eta = 1, \ldots, N)$. In the following, we will graphically analyze the collisions between two vector solitons and the energy transfer among three components.

A. Case $m = 2$ and $n = 1$

If we take $m = 2$ and $n = 1$ in solutions (A9), the two-bright-one-dark or two-bright-one-antidark vector-soliton solutions of Eq. (17) will be obtained. From the analysis in Sec. III, it can be found that the conditions for the shape-preserving and shape-changing collisions between two solitons in the q_s $(s = 1,2)$ component and conditions for

TABLE I. Six types of mixed-type vector-soliton collisions.

q_1, q_2 \ q_3	Antidark-antidark shape-preserving soliton collision	Dark-antidark shape-preserving soliton collision	Dark-dark shape-preserving soliton collision
Bright-bright shape-preserving soliton collision	case (a)	case (b)	case (c)
Bright-bright shape-changing soliton collision	case (d)	case (e)	case (f)

the dark or antidark soliton in the q_3 component are mutually independent. Therefore, we can have six types of mixed-type vector-soliton collisions (see Table I).

Here we show graphically cases (a), (e), and (f) from Table I. If we choose $\chi_{1,2}/\chi_{1,1} = \chi_{2,2}/\chi_{2,1}$ and make k_1 and k_2 both satisfy condition (13), we will obtain case (a) as shown in Fig. 1. It can be seen that two vector solitons pass through each other without any change in shape except for small shifts. This elastic collision is not affected by the appearance of antidark solitons in the third component. In order to obtain the shape-changing collision of two bright solitons in the q_s ($s = 1,2$) component and the shape-preserving collision of two dark solitons in the q_3 component, we take $\chi_{1,2}/\chi_{1,1} \neq \chi_{2,2}/\chi_{2,1}$ and k_j ($j = 1,2$) under condition (14), as shown in Fig. 2. If we set $\chi_{22} = 0$, then the amplitude of the right soliton in the q_2 component will become zero, which means that it transfers all the energy to the soliton in the q_1 component after the collision, as seen in Fig. 3. Then the amplitude of the soliton in the q_1 component will increase. This phenomenon might be used to realize the information transfer through the energy switching between the polarization components [34]. More importantly, it may be applied to the all-optical switching based on the cross-phase modulation between a signal (one vector soliton) and a control pulse (the other vector soliton) [35].

B. Case $m = 1$ and $n = 2$

Choosing $m = 1$ and $n = 2$ in solutions (A9), we can obtain the one-bright-two-dark or one-bright-two-antidark vector-soliton solutions of Eq. (17). According to the analysis in Sec. III, there is no energy exchange among those three components. If we choose both k_1 and k_2 under condition (13), the case of the shape-preserving bright-bright soliton collision in the q_1 component and the shape-preserving antidark-antidark soliton collision in the q_l ($l = 2,3$) component will be obtained, as seen in Fig. 4. Similarly, the case of the shape-preserving bright-bright soliton collision in the q_1 component and the shape-preserving antidark-dark soliton collision in the q_l ($l = 2,3$) component can be derived with k_1 and k_2 under conditions (13) and (14), respectively (see Fig. 5). Figure 6 displays the shape-preserving soliton collisions among three components with a bright-bright soliton collision in the q_1 component and a dark-dark soliton collision in the q_l ($l = 2,3$) component, with the choice of both k_1 and k_2 under condition (14).

V. NUMERICAL SIMULATIONS OF THE MIXED-TYPE VECTOR-SOLITON SOLUTIONS

To support the analytic results of the mixed-type vector solitons and analyze the stability of solutions, we perform the numerical simulations in the MATLAB environment by means of the TSS method, which can be regarded as a combination of the time-splitting discretization and Fourier spectral methods [36,37]. Such a method was first used to study the nonlinear Schrödinger equation in the semiclassical regime [36,37]. Moreover, it has been shown to be unconditionally stable, time reversible, and time-transverse invariant for the Gross-Pitaevskii equation [38].

As for Eq. (1), we choose q_ς ($\varsigma = 1,2$; $m = 1$; and $N = 2$) in solutions (A7) at $t = 0$ as the initial pulses

$$q_1(x,0) = \frac{|\chi_{1,1}|\exp(i\Phi_1)}{\sqrt{\sigma_1+\sigma_1^*+2|\sigma_1|\cosh[(k_1^*+k_1)x+\ln|\sigma_1|]}}, \quad (18a)$$

$$q_2(x,0) = |\alpha_1|\sqrt{1-\frac{\sigma_1+\sigma_1^*-\varrho_{1,1}-\varrho_{1,1}^*}{\sigma_1+\sigma_1^*+2|\sigma_1|\cosh[(k_1^*+k_1)x+\ln|\sigma_1|]}} \times \exp(i\Phi_2), \quad (18b)$$

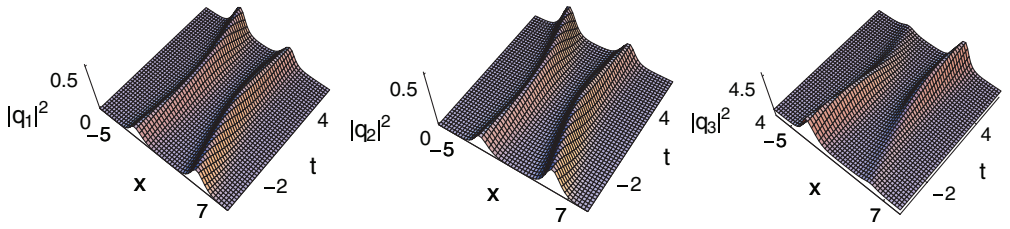

FIG. 1. (Color online) Shape-preserving collisions of two bright solitons in the q_1 and q_2 components and shape-preserving collision of two antidark solitons in the q_3 component via solutions (A9). The parameters are $\gamma = 2$, $\mu = -5$, $\alpha_1 = 2$, $k_1 = 1 + 1.8i$, $k_2 = 1 + 2.1i$, $\chi_{11} = \chi_{21} = 1$, and $\chi_{12} = \chi_{22} = 2$.

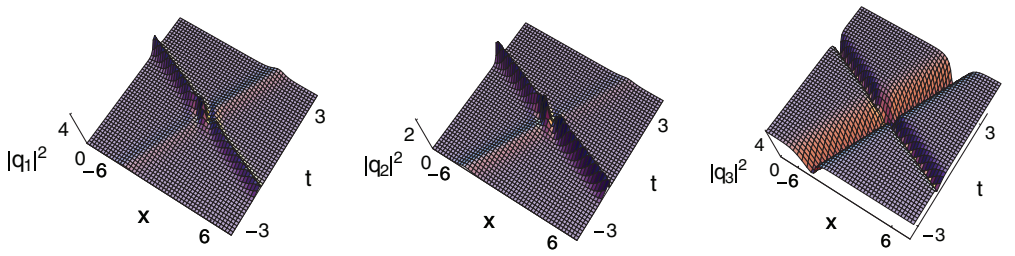

FIG. 2. (Color online) Shape-changing collision of two bright solitons in the q_1 and q_2 components and shape-preserving collision of two dark solitons in the q_3 component via solutions (A9). The parameters are $\gamma = 1, \mu = -2, \alpha_1 = 2, k_1 = 1 + 1.5i, k_2 = 1 - 1.5i, \chi_{11} = \chi_{21} = 1$, $\chi_{12} = 2 + i$, and $\chi_{22} = 1.5 - i$.

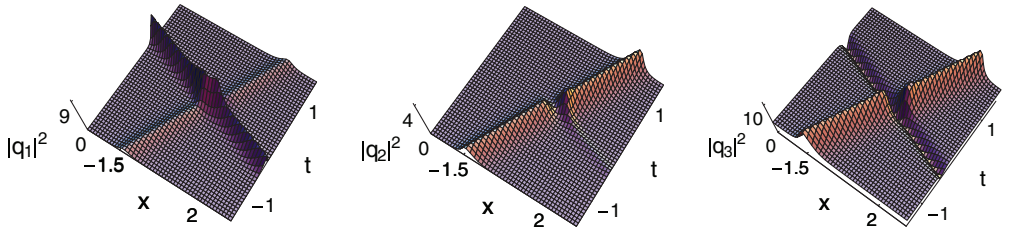

FIG. 3. (Color online) Shape-changing collision of two bright solitons in the q_1 and q_2 components and shape-preserving collision of one dark and one antidark soliton in the q_3 component via solutions (A9). The parameters are $\gamma = 1, \mu = -2, \alpha_1 = 2, k_1 = 2 + 1.5i, k_2 = 2 - 1.8i$, $\chi_{11} = \chi_{21} = 1$, $\chi_{12} = 1 + i$, and $\chi_{22} = 0$.

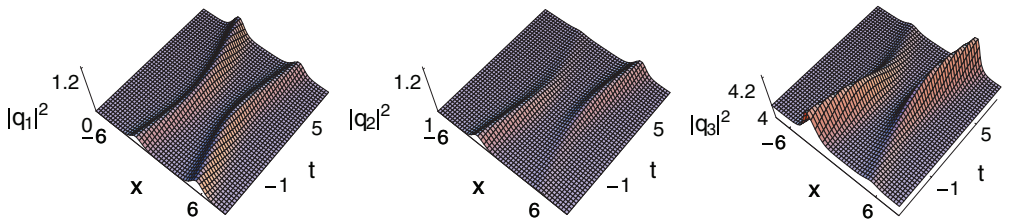

FIG. 4. (Color online) Shape-preserving collisions of two bright solitons in the q_1 component and shape-preserving collision of two antidark solitons in the q_2 and q_3 components via solutions (A9). The parameters are $\gamma = 2, \mu = -6, \alpha_1 = 1, \alpha_2 = 2, k_1 = 1 + 2.3i, k_2 = 1 + 2.65i$, $\chi_{11} = 1$, and $\chi_{12} = 2$.

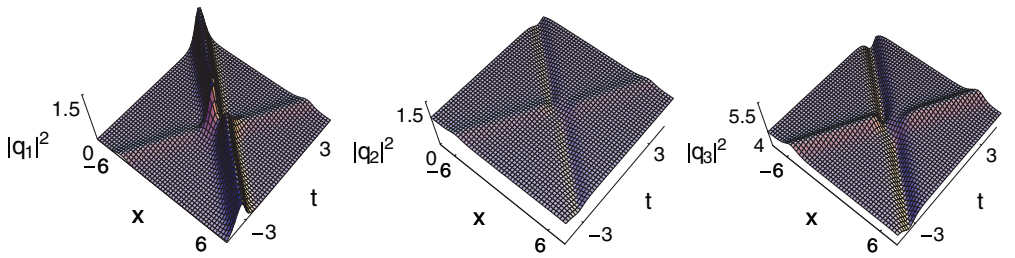

FIG. 5. (Color online) Shape-preserving collisions of two bright solitons in the q_1 component and shape-preserving collision of one dark and one antidark soliton in the q_2 and q_3 components via solutions (A9). The parameters are $\gamma = 2, \mu = -6, \alpha_1 = 1, \alpha_2 = 2, k_1 = 1 + 3i$, $k_2 = 1 + 1.5i$, $\chi_{11} = 1$, and $\chi_{12} = 2$.

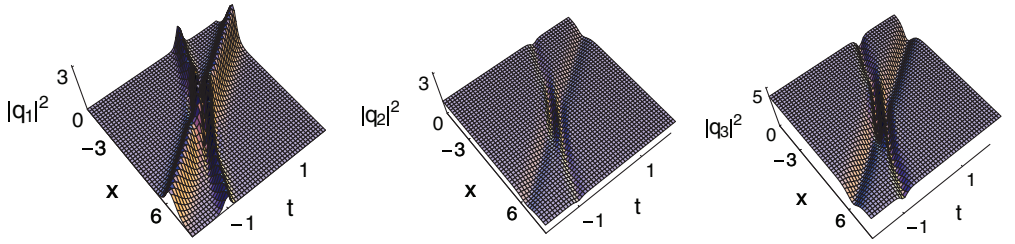

FIG. 6. (Color online) Shape-preserving collisions of two bright solitons in the q_1 component and shape-preserving collision of two dark solitons in the q_2 and q_3 components via solutions (A9). The parameters are $\gamma = 2, \mu = -6, \alpha_1 = 1, \alpha_2 = 2, k_1 = 1 + i, k_2 = 1 - 2i, \chi_{11} = 1$, and $\chi_{12} = 2$.

where

$$\Theta = \alpha_1^2\rho_2, \quad b = -\frac{1}{4}\gamma\Theta, \quad \varrho_{1,1} = -\frac{k_1\sigma_1}{k_1^*}, \quad \sigma_1 = \frac{|k_1|^2\rho_1|\chi_{1,1}|^2(4ik_1\gamma + 4\mu + 3\gamma^2\Theta)}{(k_1+k_1^*)^2[k_1^*(8k_1 - 4i\gamma\Theta) + \Theta(4ik_1\gamma + 4\mu + 3\gamma^2\Theta)]},$$

$$\Phi_1 = \frac{i(k_1^* - k_1)x}{2} + 3bx - \frac{i}{2}\ln\frac{\chi_{1,1}[1+\sigma_1^*\exp(k_1^*x + k_1x)]^3}{\chi_{1,1}^*[1+\sigma_1\exp(k_1^*x + k_1x)]^3},$$

$$\Phi_2 = 3bx - \frac{i}{2}\ln\frac{[1+\varrho_{1,1}\exp(k_1^*x + k_1x)][1+\sigma_1^*\exp(k_1^*x + k_1x)]^3}{[1+\varrho_{1,1}^*\exp(k_1^*x + k_1x)][1+\sigma_1\exp(k_1^*x + k_1x)]^3}.$$

The finite computational region of x is chosen as $[a,b]$ and the corresponding boundary conditions are $q_\varsigma(a,t) = q_\varsigma(b,t)$ $(\varsigma = 1,2)$ for $t \geqslant 0$. The mesh grid points can be given as follows:

$$x_j = a + jdx, \quad t_\tau = \tau dt, \quad j = 0,1,\ldots,M, \quad \tau = 0,1,2,\ldots, \tag{19}$$

where dx and dt are, respectively, the steps along the axes of x and t and M is an integer. Then we solve Eq. (1) in two steps from $t = t_\tau$ to $t_{\tau+1}$. The first step is solving the linear equations

$$iq_{1,t} + q_{1,xx} = 0, \tag{20a}$$
$$iq_{2,t} + q_{2,xx} = 0 \tag{20b}$$

by means of the discrete Fourier spectral method and the exact integral in t, which leads to the results

$$Q_{1,j}^{\tau+1} = \mathcal{F}_{1,j}^{-1}\left[\exp(-i\omega^2 dt)\mathcal{F}_\omega\left[Q_{1,j}^\tau\right]\right], \tag{21a}$$
$$Q_{2,j}^{\tau+1} = \mathcal{F}_{2,j}^{-1}\left[\exp(-i\omega^2 dt)\mathcal{F}_\omega\left[Q_{2,j}^\tau\right]\right], \tag{21b}$$

in which $Q_{\varsigma,j}^\tau$ $(\varsigma = 1,2)$ denotes the approximation to $q_\varsigma(x_j,t_\tau)$ $(\varsigma = 1,2)$ and ω is the frequency in the field of Fourier. In the second step we handle the sets of equations associated with the nonlinear parts

$$iq_{1,t} + \mu[(|q_1|^2 + |q_2|^2)q_1] + i\gamma[(|q_1|^2 + |q_2|^2)q_1]_x = 0, \tag{22a}$$
$$iq_{2,t} + \mu[(|q_1|^2 + |q_2|^2)q_2] + i\gamma[(|q_1|^2 + |q_2|^2)q_2]_x = 0. \tag{22b}$$

The derivative parts with respect to x are also treated via the Fourier method and Eqs. (22) are replaced by

$$Q_{1,jt} - i\mu(|Q_{1,j}|^2 + |Q_{2,j}|^2)Q_{1,j} + \gamma\mathcal{F}_{1,j}^{-1} \times [\exp(i\omega dt)\mathcal{F}_\omega[(|Q_{1,j}|^2 + |Q_{2,j}|^2)Q_{1,j}]] = 0, \tag{23a}$$
$$Q_{2,jt} - i\mu(|Q_{1,j}|^2 + |Q_{2,j}|^2)Q_{2,j} + \gamma\mathcal{F}_{1,j}^{-1} \times [\exp(i\omega dt)\mathcal{F}_\omega[(|Q_{1,j}|^2 + |Q_{2,j}|^2)Q_{2,j}]] = 0. \tag{23b}$$

Instead of using the direct integral in t, we adopt a fourth-order Runge-Kutta method [39] to obtain the recursion relationship between $Q_{\varsigma,j}^\tau$ and $Q_{\varsigma,j}^{\tau+1}$ $(\varsigma = 1,2)$. Combining the splitting steps via the standard second-order splitting, we can simulate the propagation of the mixed-type vector solitons for Eq. (1) with the specific choices of parameters.

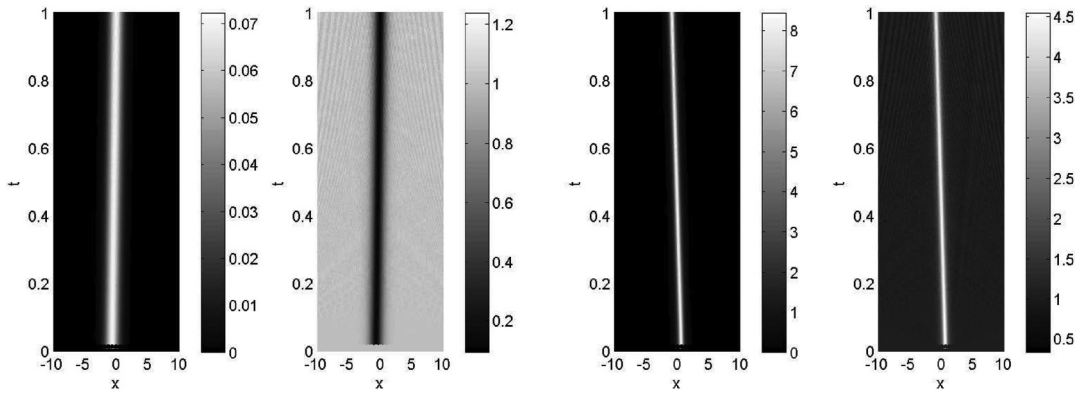

FIG. 7. Numerical simulations of the propagations of the initial pulses $q_j(x,0)$ $(j = 1,2)$. Here we choose $a = 20$, $b = -20$, $dt = 0.001$, and $M = 2^{10}$ and the iteration times are 1000. (a) The initial pulse is a bright-dark vector soliton with $\gamma = 1$, $\mu = -2.5$, $\alpha_1 = \chi_{11} = 1$, and $k_1 = 1 + 0.6i$. (b) The initial pulse is a bright-antidark vector soliton with $\gamma = 1$, $\mu = -2.5$, $\alpha_1 = \chi_{11} = 1$, and $k_1 = 1 - 0.5i$.

When we choose the parameters in solutions (18) under conditions (14), the input initial pulse will be a bright-dark vector soliton. Through the above simulation method we find that the bright-dark vector soliton can propagate stably, as seen in Fig. 7(a). Although some small oscillations arise in the background of the dark soliton, the intensity and width have almost no changes as the distance evolves. Similarly, when the initial pulse is chosen as a bright-antidark vector soliton with the parameters in solutions (18) satisfying conditions (13), the stable propagation of bright-antidark vector soliton can be obtained as seen in Fig. 7(b). If we introduce a white noise (0.1 random $[1,M]$) in the initial phases and choose the same parameters as those in Fig. 7, the pulses can also propagate stably. Therefore, the mixed-type vector solitons for Eq. (1) could resist the initial white noise perturbation and can be realized through the numerical simulations. In order to obtain general conclusions about the soliton stability, one would need to conduct a number of numerical simulations with respect to other initial perturbations using an advanced numerical method.

VI. CONCLUSION

In this paper we have studied the mixed-type vector solitons in Eq. (1) that arise in optical fibers. Via the Hirota method, we have constructed general bilinear equations of Eq. (1) in expressions (5)–(8). Mixed-type (m-bright-n-dark or m-bright-n-antidark) vector one- and two-soliton solutions in expressions (A7) and (A9) have been derived from bilinear equations (5)–(8). An asymptotic analysis of solutions (A9) has also been made to better understand the behaviors of vector solitons before and after collision. In addition, we have graphically analyzed the mixed-type vector-soliton collisions of Eq. (1) with $N=3$ and displayed the shape-preserving and shape-changing collisions of mixed-type vector solitons. Finally, a numerical simulation has been performed to support the analytic mixed-type vector-soliton solutions. Attention should be paid to the following aspects.

(i) Bilinear equations (5)–(8) of Eq. (1) are more general than those in Refs. [16,17]. Moreover, solutions (A7) can describe two types of vector solitons (m-bright–n-antidark and m-bright–n-dark vector solitons) under conditions (13)–(16).

(ii) Through the asymptotic analysis of solutions (A9), we have obtained the conditions for the shape-preserving and shape-changing (along with the energy redistribution among the components) collisions of the mixed-type vector solitons in Sec. III B. As a special case, collisions of two two-bright-one-dark or two-bright-one-antidark vector solitons (see Figs. 1–3) and two one-bright-two-dark or one-bright-two-antidark vector solitons (see Figs. 4–6) have been studied. These studies might be of certain value in information transfer and all-optical switching.

(iii) As suggested in previous studies (see, e.g., Refs. [10–13]), the bright-dark vector solitons exist only in the mixed or defocusing CNLS equations, which usually describe the propagation of picosecond pulses in optical fibers. However, because of the introduction of the higher-order nonlinear terms, the mixed-type vector solitons have nothing to do with the sign of cubic nonlinearity $\mu\rho_\eta$ ($\eta=1,\ldots,N$) and can be used as femtosecond pulses in optical fibers. We note that Ref. [14] has numerically discussed the dynamics of interacting dark-bright two-dimensional vector solitons, which can form the bound states to describe the atomic soliton molecules in quasi-two-dimensional immiscible Bose-Einstein condensates. Our analytical results on the mixed-type vector solitons in the CMDNLS equations could also be extended to the two-dimensional case and used to form the mixed-type vector-soliton bound states in the femtosecond regime of birefringent optical fibers.

ACKNOWLEDGMENTS

This work was supported by the National Natural Science Foundation of China under Grant No. 11272023, the Fundamental Research Funds for the Central Universities of China under Grant No. 2011BUPTYB02, the National Basic Research Program of China (Program No. 973) under Grant No. 2010CB923200, and by the Open Fund of State Key Laboratory of Information Photonics and Optical Communications (Beijing University of Posts and Telecommunications).

APPENDIX

1. Mixed-type vector one-soliton solutions of Eq. (1)

To obtain the mixed-type vector one-soliton solutions of Eq. (1), we terminate the power series expansions as

$$g_s=\varepsilon g_s^{(1)} \quad (s=1,\ldots,m), \tag{A1}$$

$$h_l=h_l^{(0)}\left(1+\varepsilon^2 h_l^{(2)}\right) \quad (l=1,\ldots,n), \tag{A2}$$

$$f=f^{(0)}\left(1+\varepsilon^2 f^{(2)}\right) \quad (m+n=N) \tag{A3}$$

and assume that

$$g_s^{(1)}=\chi_{s,1}\exp(\theta_1) \quad (s=1,\ldots,m), \tag{A4}$$

$$\begin{aligned} h_l^{(0)}&=\alpha_l\exp(-ia_lt),\\ h_l^{(2)}&=\varrho_{l,1}\exp(\theta_1+\theta_1^*) \quad (l=1,\ldots,n), \end{aligned} \tag{A5}$$

$$\begin{aligned} f^{(0)}&=\exp(-ibx),\\ f^{(2)}&=\sigma_1\exp(\theta_1+\theta_1^*) \quad \text{with } \theta_1=k_1x+w_1t, \end{aligned} \tag{A6}$$

where α_l ($l=1,\ldots,n$) is a real constant; $\chi_{s,1}$ ($s=1,\ldots,m$) and k_1 are complex constants; a_l ($l=1,\ldots,n$) and b are both real constants to be determined; and $\varrho_{l,1}$ ($l=1,\ldots,n$), σ_1, and w_1 are complex constants to be determined. Substituting expressions (A4)–(A6) into Eqs. (5)–(8), we have

$$\lambda=-\frac{1}{4}\sum_{l=1}^{n}\alpha_l^2\rho_{m+l}\left(4\mu+\gamma^2\sum_{l=1}^{n}\alpha_l^2\rho_{m+l}\right).$$

Without loss of generality we set $\varepsilon=1$ and derive the mixed-type vector one-soliton solutions of Eq. (1) as

follows:

$$q_s = \frac{|\chi_{s,1}|\exp(i\Phi_s)}{\sqrt{\sigma_1+\sigma_1^*+2|\sigma_1|\cosh(\theta_1+\theta_1^*+\ln|\sigma_1|)}} \quad (s=1,\ldots,m), \tag{A7a}$$

$$q_{m+l} = |\alpha_l|\sqrt{1-\frac{\sigma_1+\sigma_1^*-\varrho_{l,1}-\varrho_{l,1}^*}{\sigma_1+\sigma_1^*+2|\sigma_1|\cosh(\theta_1+\theta_1^*+\ln|\sigma_1|)}}\exp(i\Phi_{m+l}) \quad (l=1,\ldots,n), \tag{A7b}$$

where

$$\Theta=\sum_{l=1}^{n}\alpha_l^2\rho_{m+l}, \quad a_l=-\frac{1}{16}\Theta(16\mu+3\gamma^2\Theta), \quad b=-\frac{1}{4}\gamma\Theta,$$

$$\sigma_1=\frac{|k_1|^2\sum_{s=1}^{m}\rho_s|\chi_{s,1}|^2(4ik_1\gamma+4\mu+3\gamma^2\Theta)}{(k_1+k_1^*)^2[k_1^*(8k_1-4i\gamma\Theta)+\Theta(4ik_1\gamma+4\mu+3\gamma^2\Theta)]},$$

$$\varrho_{l,1}=-\frac{k_1\sigma_1}{k_1^*}, \quad w_1=ik_1^2+\frac{1}{16}\Theta(8k_1\gamma+16i\mu+3i\gamma^2\Theta),$$

$$\Phi_s=\frac{i(\theta_1^*-\theta_1)}{2}+3bx-\frac{i}{2}\ln\frac{\chi_{s,1}[1+\sigma_1^*\exp(\theta_1+\theta_1^*)]^3}{\chi_{s,1}^*[1+\sigma_1\exp(\theta_1+\theta_1^*)]^3}, \quad m+n=N,$$

$$\Phi_{m+l}=-a_lt+3bx-\frac{i}{2}\ln\frac{[1+\varrho_{l,1}\exp(\theta_1+\theta_1^*)][1+\sigma_1^*\exp(\theta_1+\theta_1^*)]^3}{[1+\varrho_{l,1}^*\exp(\theta_1+\theta_1^*)][1+\sigma_1\exp(\theta_1+\theta_1^*)]^3}.$$

2. Mixed-type vector two-soliton solutions of Eq. (1)

Similar to the procedure above, substituting the expansions of g_s $(s=1,\ldots,m)$, h_l $(m=1,\ldots,n)$, and f as

$$g_s=\varepsilon g_s^{(1)}+\varepsilon^3 g_s^{(3)} \quad (s=1,\ldots,m), \tag{A8a}$$

$$h_l=h_l^{(0)}\left(1+\varepsilon^2 h_l^{(2)}+\varepsilon^4 h_l^{(4)}\right) \quad (l=1,\ldots,n), \tag{A8b}$$

$$f=f^{(0)}(1+\varepsilon^2 f^{(2)}+\varepsilon^4 f^{(4)}) \quad (m+n=N) \tag{A8c}$$

into Eqs. (5)–(8), we get the mixed-type vector two-soliton solutions of Eq. (1)

$$q_s=\Omega[\chi_{s,1}\exp(\theta_1)+\chi_{s,2}\exp(\theta_2)+\chi_{s,3}\exp(\theta_1+\theta_1^*+\theta_2)+\chi_{s,4}\exp(\theta_2+\theta_2^*+\theta_1)], \tag{A9a}$$

$$\begin{aligned}q_{m+l}=\Omega\alpha_l\exp(-ia_lz)[&1+\varrho_{l,1}\exp(\theta_1+\theta_1^*)+\varrho_{l,2}\exp(\theta_2+\theta_2^*)+\varrho_{l,3}\exp(\theta_1+\theta_2^*)\\&+\varrho_{l,4}\exp(\theta_2+\theta_1^*)+\varrho_{l,5}\exp(\theta_1+\theta_2+\theta_1^*+\theta_2^*)],\end{aligned} \tag{A9b}$$

with

$$\theta_1=k_1x+w_1t, \quad w_1=ik_1^2+\frac{1}{16}\Theta(8k_1\gamma+16i\mu+3i\gamma^2\Theta),$$

$$\theta_2=k_2x+w_2t, \quad w_2=ik_2^2+\frac{1}{16}\Theta(8k_2\gamma+16i\mu+3i\gamma^2\Theta),$$

$$\chi_{s,3}=-\frac{(k_1-k_2)[k_1\sigma_1\chi_{s,2}-k_2\sigma_4\chi_{s,1}+k_1^*(\chi_{s,2}\sigma_1-\chi_{s,1}\sigma_4)]}{(k_1+k_1^*)(k_2+k_1^*)},$$

$$\chi_{s,4}=-\frac{(k_1-k_2)[-k_2\sigma_2\chi_{s,1}+k_1\sigma_3\chi_{s,2}-k_2^*(\sigma_2\chi_{s,1}-\sigma_3\chi_{s,2})]}{(k_1+k_2^*)(k_2+k_2^*)},$$

$$\sigma_1=\frac{|k_1|^2\sum_{s=1}^{m}\rho_s|\chi_{s,1}|^2(4ik_1\gamma+4\mu+3\gamma^2\Theta)}{(k_1+k_1^*)^2[k_1^*(8k_1-4i\gamma\Theta)+\Theta(4ik_1\gamma+4\mu+3\gamma^2\Theta)]},$$

$$\sigma_2=\frac{|k_2|^2\sum_{s=1}^{m}\rho_s|\chi_{s,2}|^2(4ik_2\gamma+4\mu+3\gamma^2\Theta)}{(k_2+k_2^*)^2[k_2^*(8k_2-4i\gamma\Theta)+\Theta(4ik_2\gamma+4\mu+3\gamma^2\Theta)]},$$

$$\sigma_3=\frac{k_1k_2^*\sum_{s=1}^{m}\rho_s\chi_{s,1}\chi_{s,2}^*(4ik_1\gamma+4\mu+3\gamma^2\Theta)}{(k_1+k_2^*)^2[k_2^*(8k_1-4i\gamma\Theta)+\Theta(4ik_1\gamma+4\mu+3\gamma^2\Theta)]},$$

$$\sigma_4 = \frac{k_2 k_1^* \sum_{s=1}^{m} \rho_s \chi_{s,2} \chi_{s,1}^* (4ik_2\gamma + 4\mu + 3\gamma^2\Theta)}{(k_2 + k_1^*)^2 [k_1^*(8k_2 - 4i\gamma\Theta) + \Theta(4ik_2\gamma + 4\mu + 3\gamma^2\Theta)]},$$

$$\sigma_5 = -\frac{(k_1^* - k_2^*)[k_2(\sigma_3\chi_{s,3} - \sigma_1\chi_{s,4}) + \sigma_3\chi_{s,3}k_1^* - \sigma_1\chi_{s,4}k_2^*]}{\chi_{s,1}(k_2 + k_1^*)(k_2 + k_2^*)},$$

$$\varrho_{l,1} = -\frac{k_1\sigma_1}{k_1^*}, \quad \varrho_{l,2} = -\frac{k_2\sigma_2}{k_2^*}, \quad \varrho_{l,3} = -\frac{k_1\sigma_3}{k_2^*}, \quad \varrho_{l,4} = -\frac{k_2\sigma_4}{k_1^*}, \quad \varrho_{l,5} = \frac{k_1 k_2 \sigma_5}{k_1^* k_2^*},$$

$$\begin{aligned}\Omega = {} & \exp(ibx)[1 + \sigma_1^* \exp(\theta_1 + \theta_1^*) + \sigma_2^* \exp(\theta_2 + \theta_2^*) + \sigma_3^* \exp(\theta_1 + \theta_2^*) + \sigma_4^* \exp(\theta_2 + \theta_1^*) \\ & + \sigma_5^* \exp(\theta_1 + \theta_2 + \theta_1^* + \theta_2^*)]/\{\exp(-ibx)[1 + \sigma_1 \exp(\theta_1 + \theta_1^*) + \sigma_2 \exp(\theta_2 + \theta_2^*) \\ & + \sigma_3 \exp(\theta_1 + \theta_2^*) + \sigma_4 \exp(\theta_2 + \theta_1^*) + \sigma_5 \exp(\theta_1 + \theta_2 + \theta_1^* + \theta_2^*)]\}^2 \\ & (s = 1, \ldots, m; l = 1, \ldots, n).\end{aligned}$$

3. Asymptotic analysis of solutions (A9)

The asymptotic expressions of vector solitons before and after collisions can be given as follows: For S^{1-} ($\theta_1 + \theta_1^* \sim 0$, $\theta_2 + \theta_2^* \to -\infty$),

$$q_s \to S_s^{1-} = \frac{|\chi_{s,1}| \exp(i\Phi_{1,s}^-)}{\sqrt{\sigma_1 + \sigma_1^* + 2|\sigma_1| \cosh(\theta_1 + \theta_1^* + \ln|\sigma_1|)}}, \tag{A10a}$$

$$\begin{aligned}q_{m+l} \to S_{m+l}^{1-} = {} & |\alpha_l| \sqrt{1 - \frac{\sigma_1 + \sigma_1^* - \varrho_{l,1} - \varrho_{l,1}^*}{\sigma_1 + \sigma_1^* + 2|\sigma_1| \cosh(\theta_1 + \theta_1^* + \ln|\sigma_1|)}} \exp(i\Phi_{1,m+l}^-) \\ & (s = 1, \ldots, m; l = 1, \ldots, n),\end{aligned} \tag{A10b}$$

with

$$\Phi_{1,s}^- = \frac{i(\theta_1^* - \theta_1)}{2} + 3bx - \frac{i}{2} \ln \frac{\chi_{s,1}[1 + \sigma_1^* \exp(\theta_1 + \theta_1^*)]^3}{\chi_{s,1}^*[1 + \sigma_1 \exp(\theta_1 + \theta_1^*)]^3},$$

$$\Phi_{1,m+l}^- = -a_l t + 3bx - \frac{i}{2} \ln \frac{[1 + \varrho_{l,1}\exp(\theta_1 + \theta_1^*)][1 + \sigma_1^* \exp(\theta_1 + \theta_1^*)]^3}{[1 + \varrho_{l,1}^* \exp(\theta_1 + \theta_1^*)][1 + \sigma_1 \exp(\theta_1 + \theta_1^*)]^3};$$

for $S^{2-}(\theta_2 + \theta_2^* \sim 0, \theta_1 + \theta_1^* \to \infty)$,

$$q_s \to S_s^{2-} = \frac{\left|\frac{\chi_{s,3}}{\sigma_1}\right| \exp(i\Phi_{2,s}^-)}{\sqrt{\frac{\sigma_5}{\sigma_1} + \frac{\sigma_5^*}{\sigma_1^*} + 2\left|\frac{\sigma_5}{\sigma_1}\right| \cosh\left(\theta_2 + \theta_2^* + \ln\left|\frac{\sigma_5}{\sigma_1}\right|\right)}}, \tag{A11a}$$

$$\begin{aligned}q_{m+l} \to S_{m+l}^{2-} = {} & \left|\frac{\alpha_l \varrho_{l,1}}{\sigma_1}\right| \sqrt{1 - \frac{\frac{\sigma_5}{\sigma_1} + \frac{\sigma_5^*}{\sigma_1^*} - \frac{\varrho_{l,5}}{\varrho_{l,1}} - \frac{\varrho_{l,5}^*}{\varrho_{l,1}^*}}{\frac{\sigma_5}{\sigma_1} + \frac{\sigma_5^*}{\sigma_1^*} + 2\left|\frac{\sigma_5}{\sigma_1}\right| \cosh\left(\theta_2 + \theta_2^* + \ln\left|\frac{\sigma_5}{\sigma_1}\right|\right)}} \exp(i\Phi_{2,m+l}^-) \\ & (s = 1, \ldots, m; l = 1, \ldots, n),\end{aligned} \tag{A11b}$$

with

$$\Phi_{2,s}^- = \frac{i(\theta_2^* - \theta_2)}{2} + 3bx - \frac{i}{2} \ln \frac{\chi_{s,3}[\sigma_1^* + \sigma_5^* \exp(\theta_2 + \theta_2^*)]^3}{\chi_{s,3}^*[\sigma_1 + \sigma_5 \exp(\theta_2 + \theta_2^*)]^3},$$

$$\Phi_{2,m+l}^- = -a_l t + 3bx - \frac{i}{2} \ln \frac{[\varrho_{l,1} + \varrho_{l,5}\exp(\theta_2 + \theta_2^*)][\sigma_1^* + \sigma_5^* \exp(\theta_2 + \theta_2^*)]^3}{[\varrho_{l,1}^* + \varrho_{l,5}^* \exp(\theta_2 + \theta_2^*)][\sigma_1 + \sigma_5 \exp(\theta_2 + \theta_2^*)]^3};$$

for $S^{1+}(\theta_1 + \theta_1^* \sim 0, \theta_2 + \theta_2^* \to \infty)$,

$$q_s \to S_s^{1+} = \frac{\left|\frac{\chi_{s,4}}{\sigma_2}\right| \exp(i\Phi_{1,s}^+)}{\sqrt{\frac{\sigma_5}{\sigma_2} + \frac{\sigma_5^*}{\sigma_2^*} + 2\left|\frac{\sigma_5}{\sigma_2}\right| \cosh\left(\theta_1 + \theta_1^* + \ln\left|\frac{\sigma_5}{\sigma_2}\right|\right)}}, \tag{A12a}$$

$$\begin{aligned}q_{m+l} \to S_{m+l}^{1+} = {} & \left|\frac{\alpha_l \varrho_{l,2}}{\sigma_2}\right| \sqrt{1 - \frac{\frac{\sigma_5}{\sigma_2} + \frac{\sigma_5^*}{\sigma_2^*} - \frac{\varrho_{l,5}}{\varrho_{l,2}} - \frac{\varrho_{l,5}^*}{\varrho_{l,2}^*}}{\frac{\sigma_5}{\sigma_2} + \frac{\sigma_5^*}{\sigma_2^*} + 2\left|\frac{\sigma_5}{\sigma_2}\right| \cosh\left(\theta_1 + \theta_1^* + \ln\left|\frac{\sigma_5}{\sigma_2}\right|\right)}} \exp(i\Phi_{1,m+l}^+) \\ & (s = 1, \ldots, m; l = 1, \ldots, n),\end{aligned} \tag{A12b}$$

with

$$\Phi_{1,s}^{+}=\frac{i(\theta_1^*-\theta_1)}{2}+3bx-\frac{i}{2}\ln\frac{\chi_{s,4}[\sigma_2^*+\sigma_5^*\exp(\theta_1+\theta_1^*)]^3}{\chi_{s,4}^*[\sigma_2+\sigma_5\exp(\theta_1+\theta_1^*)]^3},$$

$$\Phi_{1,m+l}^{+}=-a_l t+3bx-\frac{i}{2}\ln\frac{[\varrho_{l,2}+\varrho_{l,5}\exp(\theta_1+\theta_1^*)][\sigma_2^*+\sigma_5^*\exp(\theta_1+\theta_1^*)]^3}{[\varrho_{l,2}^*+\varrho_{l,5}^*\exp(\theta_1+\theta_1^*)][\sigma_2+\sigma_5\exp(\theta_1+\theta_1^*)]^3};$$

and for $S^{2+}(\theta_2+\theta_2^*\sim 0,\theta_1+\theta_1^*\to-\infty)$,

$$q_s\to S_s^{2+}=\frac{|\chi_{s,2}|\exp(i\Phi_{2,s}^{+})}{\sqrt{\sigma_2+\sigma_2^*+2|\sigma_2|\cosh(\theta_2+\theta_2^*+\ln|\sigma_2|)}}, \tag{A13a}$$

$$q_{m+l}\to S_{m+l}^{2+}=|\alpha_l|\sqrt{1-\frac{\sigma_2+\sigma_2^*-\varrho_{l,2}-\varrho_{l,2}^*}{\sigma_2+\sigma_2^*+2|\sigma_2|\cosh(\theta_2+\theta_2^*+\ln|\sigma_2|)}}\exp(i\Phi_{2,m+l}^{+})$$

$$(s=1,\ldots,m;l=1,\ldots,n), \tag{A13b}$$

with

$$\Phi_{2,s}^{+}=\frac{i(\theta_2^*-\theta_2)}{2}+3bx-\frac{i}{2}\ln\frac{\chi_{s,2}[1+\sigma_2^*\exp(\theta_2+\theta_2^*)]^3}{\chi_{s,2}^*[1+\sigma_2\exp(\theta_2+\theta_2^*)]^3},$$

$$\Phi_{2,m+l}^{+}=-a_l t+3bx-\frac{i}{2}\ln\frac{[1+\varrho_{l,2}\exp(\theta_2+\theta_2^*)][1+\sigma_2^*\exp(\theta_2+\theta_2^*)]^3}{[1+\varrho_{l,2}^*\exp(\theta_2+\theta_2^*)][1+\sigma_2\exp(\theta_2+\theta_2^*)]^3},$$

where $S^{j\mp}$ $(j=1,2)$ denotes the status of the jth solitons before $(-)$ and after $(+)$ the collisions, respectively.

[1] Y. S. Kivshar and G. P. Agrawal, *Optical Solitons from Fibers to Photonic Crystals* (Academic, New York, 2003).
[2] C. R. Menyuk, Opt. Lett. **12**, 614 (1987).
[3] C. R. Menyuk, J. Opt. Soc. Am. B **5**, 392 (1988).
[4] R. Radhakrishnan, P. T. Dinda, and G. Millot, Phys. Rev. E **69**, 046607 (2004).
[5] T. Kanna, M. Lakshmanan, P. T. Dinda, and N. Akhmediev, Phys. Rev. E **73**, 026604 (2006).
[6] R. Radhakrishnan, M. Lakshmanan, and J. Hietarinta, Phys. Rev. E **56**, 2213 (1997).
[7] C. Anastassiou, M. Segev, K. Steiglitz, J. A. Giordmaine, M. Mitchell, M. F. Shih, S. Lan, and J. Martin, Phys. Rev. Lett. **83**, 2332 (1999).
[8] S. Trillo and W. Toruellas, *Spatial Solitons* (Springer, Berlin, 2001).
[9] A. A. Sukhorukov and Yu. S. Kivshar, *Nonlinear Guided Waves and Their Applications*, OSA Technical Digest (OSA, Washington, DC, 2001).
[10] M. Vijayajayanthi, T. Kanna, and M. Lakshmanan, Eur. Phys. J. Spec. Top. **173**, 57 (2009).
[11] M. Vijayajayanthi, T. Kanna, and M. Lakshmanan, Phys. Rev. A **77**, 013820 (2008).
[12] Y. S. Kivshar, Opt. Lett. **17**, 1322 (1992).
[13] Y. Ohta, D. S. Wang, and J. K. Yang, Stud. Appl. Math. **127**, 345 (2011).
[14] C. Y. Yin, N. G. Berloff, V. M. Pérez-García, D. Novoa, A. V. Carpentier, and H. Michinel, Phys. Rev. A **83**, 051605 (2011).
[15] M. Hisakado, T. Lizuka, and M. Wadati, J. Phys. Soc. Jpn. **63**, 2887 (1994).
[16] H. Q. Zhang, B. Tian, X. Lü, H. Li, and X. H. Meng, Phys. Lett. A **373**, 4315 (2009).
[17] M. Li, T. Bo, W. J. Liu, Y. Jiang, and K. Sun, Eur. Phys. J. D **59**, 279 (2010).
[18] Yu. S. Kivshar, V. V. Afansjev, and A. W. Snyder, Opt. Commun. **126**, 348 (1996); D. J. Frantzeskakis, J. Phys. A **29**, 3631 (1996); H. E. Nistazakis, D. J. Frantzeskakis, P. S. Balourdos, and A. Tsigopoulos, Phys. Lett. A **278**, 68 (2000).
[19] M. Hisakado and M. Wadati, J. Phys. Soc. Jpn. **64**, 408 (1995).
[20] D. Anderson and M. Lisak, Opt. Lett. **7**, 394 (1982).
[21] G. P. Agrawal, *Nonlinear Fiber Optics*, 4th ed. (Academic, New York, 2006); G. P. Agrawal, P. L. Baldeck, and R. R. Alfano, Phys. Rev. A **39**, 3406 (1989).
[22] A. C. Scott, Phys. Scr. **29**, 279 (1984).
[23] E. P. Bashkin and A. V. Vagov, Phys. Rev. B **56**, 6207 (1997).
[24] M. R. Gupta, B. K. Som, and B. Dasgupta, J. Plasma Phys. **25**, 499 (1981).
[25] H. C. Morris and R. K. Dodd, Phys. Scr. **20**, 505 (1979).
[26] G. Q. Meng, Y. T. Gao, X. Yu, Y. J. Shen, and Y. Qin, Phys. Scr. **85**, 055010 (2012); Nonl. Dyn. **70**, 609 (2012); X. Yu, Y. T. Gao, Z. Y. Sun, and Y. Liu, Phys. Rev. E **83**, 056601 (2011); Nonl. Dyn. **67**, 1023 (2012).
[27] Z. Y. Sun, Y. T. Gao, X. Yu, and Y. Liu, Europhys. Lett. **93**, 40004 (2011); Z. Y. Sun, Y. T. Gao, Y. Liu, and X. Yu, Phys. Rev. E **84**, 026606 (2011); Z. Y. Sun, Y. T. Gao, X. Yu, W. J. Liu, and Y. Liu, *ibid.* **80**, 066608 (2009).
[28] H. Q. Zhang, T. Xu, J. Li, and B. Tian, Phys. Rev. E **77**, 026605 (2008).
[29] T. Xu, B. Tian, L. L. Li, X. Lü, and C. Zhang, Phys. Plasmas **15**, 102307 (2008).
[30] W. P. Hong, Phys. Lett. A **361**, 520 (2007); B. Tian and Y. T. Gao, *ibid.* **340**, 243 (2005); **340**, 449 (2005); **362**, 283 (2007).

[31] Y. T. Gao and B. Tian, Phys. Lett. A **349**, 314 (2006); **361**, 523 (2007); Phys. Plasmas **13**, 112901 (2006).
[32] R. Hirota, *The Direct Method in Soliton Theory* (Cambridge University Press, Cambridge, 2004).
[33] W. Hereman and W. Zhuang, Acta Appl. Math. **39**, 361 (1995).
[34] C. Anastassiou, J. W. Fleisher, T. Carmon, M. Segev, and K. Steiglitz, Opt. Lett. **26**, 1498 (2001).
[35] J. E. Sharping, M. Fiorentino, P. Kumar, and R. S. Windeler, IEEE Photon. Tech. Lett. **14**, 77 (2002); A. Demircan, Sh. Amiranashvili, and G. Steinmeyer, Phys. Rev. Lett. **106**, 163901 (2011).
[36] W. Bao, S. Jin, and P. A. Markowich, J. Comput. Phys. **175**, 487 (2002).
[37] W. Bao, S. Jin, and P. A. Markowich, SIAM J. Sci. Comput. **25**, 27 (2003).
[38] W. Bao, D. Jaksch, and P. A. Markowich, J. Comput. Phys. **187**, 318 (2003).
[39] B. F. Sanders, N. D. Katopodes, and J. P. Boyd, J. Hydraul. Eng. **124**, 1 (1998).